

Phase engineering, modulational instability, and solitons of Gross–Pitaevskii-type equations in 1 + 1 dimensions

E. Kengne,^{1,2,3} A. Lakhssassi,² W. M. Liu,¹ and R. Vaillancourt³

¹*National Laboratory for Condensed Matter Physics, Institute of Physics, Chinese Academy of Sciences, Beijing 100190, People's Republic of China*

²*Département d'informatique et d'ingénierie, Université du Québec en Outaouais, 101 St-Jean-Bosco, Succursale Hull, Gatineau (PQ) J8Y 3G5, Canada*

³*Department of Mathematics and Statistics, Faculty of Science, University of Ottawa, 585 King Edward Avenue, Ottawa ON K1N 6N5, Canada*

(Received 7 October 2012; revised manuscript received 17 December 2012; published 22 February 2013)

Motivated by recent proposals of “collisionally inhomogeneous” Bose–Einstein condensates (BECs), which have a spatially modulated scattering length, we introduce a phase imprint into the macroscopic order parameter governing the dynamics of BECs with spatiotemporal varying scattering length described by a cubic Gross–Pitaevskii (GP) equation and then suitably engineer the imprinted phase to generate the modified GP equation, also called the cubic derivative nonlinear Schrödinger (NLS) equation. This equation describes the dynamics of condensates with two-body (attractive and repulsive) interactions in a time-varying quadratic external potential. We then carry out a theoretical analysis which invokes a lens-type transformation that converts the cubic derivative NLS equation into a modified NLS equation with only explicit temporal dependence. Our analysis suggests a particular interest in a specific time-varying potential with the strength of the magnetic trap $\sim 1/(t + t^*)^2$. For a time-varying quadratic external potential of this kind, an explicit expression for the growth rate of a purely growing modulational instability is presented and analyzed. We point out the effect of the imprint parameter and the parameter t^* on the instability growth rate, as well as on the solitary waves of the BECs.

DOI: [10.1103/PhysRevE.87.022914](https://doi.org/10.1103/PhysRevE.87.022914)

PACS number(s): 05.45.Yv, 03.75.Kk, 03.75.Lm, 42.65.Sf

I. INTRODUCTION

Since the realization of Bose–Einstein condensates (BECs) trapped in optical lattices, intense experimental and theoretical studies have been carried out in the fields of bright and dark matter wave solitons, coherent structures, nonlinear excitations of BEC matter waves, and modulational instability (MI) [1–18]. Appearing in many nonlinear dispersive systems [19–21], MI is a general feature of continuum as well as of discrete nonlinear wave equations. It indicates that, due to the interplay between nonlinearity and the dispersive effects, a small perturbation on the envelope of a plane wave may induce an exponential growth of the wave amplitude, resulting in the carrier-wave breakup into a train of localized waves [22]. In other words, MI causes an exponential growth of small perturbations of a carrier wave which is a result of the interplay between dispersion and nonlinearity. Studies related to MI have attracted much interest: Carr *et al.* [8] have studied analytically and numerically the MI of a nonuniform initial state in the presence of a harmonic potential in the context of a mean-field approximation BEC. Some years ago, Rapti *et al.* [12] examined the modulational and parametric instabilities arising in a nonautonomous, discrete nonlinear Schrödinger equation setup for a deep optical lattice in the BEC context; Kourakis *et al.* [23] examined the MI for the collision of two BECs in the absence of a three body interaction potential. The evolution of matter waves in time-dependent traps has been addressed, and the MI of a one-dimensional (1D) BEC system in a time-dependent harmonic potential has been investigated [24]. More recently, Mohamadou [25] investigated the MI of BECs with a time-dependent complicated potential. The MI of the Gross–Pitaevskii (GP)

equation with a time-varying harmonic potential in the case of focusing nonlinearities has been investigated in Ref. [18].

The MI for a Bose-Einstein condensate with two-body or with both two- and three-body interatomic interactions has been intensively investigated (cf. Refs. [12,18,23–25], for example); in this work we investigate the MI for BECs using the derivative cubic GP equation

$$i \frac{\partial \phi}{\partial t} + \left[\frac{\partial^2}{\partial x^2} + \tilde{V} + \tilde{g} |\phi|^2 \right] \phi + i \tilde{\beta} \frac{\partial(\phi^2 \phi^*)}{\partial x} = 0 \quad (1)$$

in which the derivative cubic terms represents the delayed nonlinear response of the system. Equation of type (1) is well known in plasma physics. It describes the evolution of small but finite amplitude Alphen waves propagating quasiparallel to a magnetic field in a low β plasma [26]. Ten years ago, an equation of the same type was found to describe the behavior of large-amplitude magnetohydrodynamic waves propagating in an arbitrary direction with respect to the magnetic field in a high β plasma [27]. Also in nonlinear optics for the propagation of very short pulses the typical Kerr nonlinearity has to be supplemented with a derivative term [28]. In the absence of the external potential, i.e., when $\tilde{V} = 0$, Eq. (1) reduces to the well known integrable derivative cubic nonlinear Schrödinger (NLS) equation in nonlinear optics derived from the mixed NLS equation through U(1)-gauge transformation [29]. The derivative cubic NLS equation also arises as the envelope equation for a weakly subcritical bifurcation to counterpropagating waves, which is also of importance in the theory interaction behavior, including complete interpenetration as well as partial annihilation, for collision between localized solutions corresponding to a single

particle and to a two particle state (cf. [30,31]). Naturally, two questions arise: (1) How should one introduce a GP model describing the impact of the cubic derivative nonlinearity interactions on the condensates? (2) How far may the derivative cubic term of the GP equation affect the MI of BECs?

The present work is motivated by the works of Refs. [18,25] and by the lack of using the derivative cubic GP equation for investigating the MI for BEC. Its main purpose is to answer the above two questions. We first introduce a phase imprint into the macroscopic order parameter governing the dynamics of BECs with a spatiotemporal s -wave scattering length in a time-dependent harmonic trapping potential described by a cubic GP equation with distributed coefficients and then engineer the imprinted phase suitably to generate a derivative cubic GP equation of form (1) (which in the rest of the paper is called the modified GP equation). The phase imprinting technique is a relatively new control and analysis tool for wave function engineering of BECs. This technique could be extended to the control of wave function amplitude, with the use of near-resonant laser frequencies to induce absorption. The phase imprinting for a BEC consists of modifying the phase distribution of the BEC, for example, by exposing it to pulsed, off-resonant laser light with a given intensity pattern. In this process, the atoms experience a spatially varying light-shift potential and acquire a corresponding phase (cf. Refs. [14,16,32] for more explanation). One of the advantages of using the technique of phase imprinting for BECs is that it does not affect the number of atoms of the condensate. Second, we used the obtained modified GP equation to give the simple treatment of MI for a single BEC. With the help of linear stability analysis (LSA), the analytical expression of the dispersion relation which is appropriate for investigating the MI of constant amplitude of the (1+1)D single BEC is established. Then, we obtain from the dispersion relation the explicit expression for the growth rate of the instability which allowed us to bring out the effect of derivative terms on the MI. Finally, we present explicit, analytical solution to describe the dynamics of a solitary waves for derivative cubic GP equation with spatiotemporal s -wave scattering length in a time-dependent harmonic trapping potential. Thus, the aim of this paper is to investigate, via the derivative cubic GP equation, the MI of the quasi-1D GP equation for the BEC with spatiotemporal s -wave scattering length in time-varying harmonic trapping potential.

The rest of the work is organized as follows: The basic formalism is given in Sec. II. In Sec. III, a generalized phase imprint transformation is used to modify a cubic GP equation into a cubic derivative GP equation; here, we investigate the MI of the cubic derivative NLS equation without external potential. The MI of the modified GP equation is investigated in Sec. IV. An attempt of finding analytical solitary-wave-like solutions of the modified GP model is carried out in Sec. V, and the main results are summarized in Sec. VI.

II. BASIC FORMALISM

The well-known Feshbach resonances are used to control the nonlinearities of matter waves by manipulating the scattering length either in time or space or in time and space, and have led to the proposal of many novel nonlinear

phenomena [4,6,33–35]. Theoretical studies have predicted that a time-dependent modulation of the scattering length can be used to stabilize attractive 2D BECs against collapse [36,37] or create robust matter-wave breathers in 1D BECs [17,38]. It has been recently found that atomic matter waves exhibit novel features under the influence of a spatially varying scattering length and, consequently, a spatially varying nonlinearity [39]. More recently, the interplay of nonlinear and linear potentials has been examined in both continuum and discrete settings [40].

The evolution of the macroscopic wave function $u(x,t)$ of the condensates is described by an inhomogeneous NLS equation called a mean-field GP equation. The inhomogeneity can be attributed to both the trapping potential and the nonlinear interaction between the atoms in the condensates. When the transverse confinement is too tight to allow scattering to the excited states of the harmonic trap in the transverse direction, the effective 1D GP equation in an expulsive harmonic trap is written as [17,41–46]

$$i \frac{\partial u(x,t)}{\partial t} + \left[\frac{\partial^2}{\partial x^2} + g(x,t) |u(x,t)|^2 + V(x,t) \right] u(x,t) = 0. \quad (2)$$

In this equation, time t and coordinate x are measured in units $2/\omega_{\perp}$ and a_{\perp} , respectively, where $a_{\perp} = (\hbar/m\omega_{\perp})^{1/2}$ and $a_0 = (\hbar/m\omega_0)^{1/2}$ are linear oscillator lengths in the transverse and cigar-axis directions, respectively. Here ω_{\perp} is the harmonic oscillator (or radial-oscillation) frequency and a_{\perp} is the corresponding linear oscillator length (in the transverse direction). The numbers ω_0 and a_0 denote the axial-oscillation frequency and the corresponding linear oscillator length, respectively, both in the cigar-axis direction. Here, m is the atomic mass. The spatiotemporal parameter $g(x,t)$ of the cubic nonlinearity represents the two-body interatomic interaction coefficient, negative for repulsive interatomic interactions (or defocusing nonlinearities) and positive for attractive ones (focusing nonlinearities). The normalized spatially and temporally modulated coefficient parameter $g(x,t)$ is proportional to the collision scattering length [36]. The sign and magnitude of $g(x,t)$ can both be changed using Feshbach resonances, which make it possible (in principle) to manipulate the sign and strength of atomic interactions [33]. It is also possible to vary the scattering length and consequently the nonlinearity coefficient $g(x,t)$ in space and time by tuning an external field in the vicinity of a Feshbach resonance [39]. The macroscopic wave function $u(x,t)$ of the condensate is normalized in units $\sqrt{\frac{8\pi g_0 \hbar}{m\omega_{\perp}}}$. Equation (2) possesses two integrals of motion: the normalized number of atoms $N = \int_{-\infty}^{+\infty} |u(x,t)|^2 dx$, and the Hamiltonian. In Eq. (2), $V(x,t)$ is the external potential. In the context that Eq. (2) describes the evolution of the wave function of a quasi-one-dimensional cigar-shaped BEC, we will consider the time-varying harmonic potential

$$V(x,t) = -\alpha(t)x^2, \quad (3)$$

which is relevant, in particular, to experimental setups in which the (magnetic) trap is strongly confined in the two directions, while it is much shallower in the third one [17,47]. The strength of the magnetic trap $\alpha(t)$ may be negative (confining potential) or positive (repulsive potential). The prefactor $\alpha(t)$

is typically fixed in current experiments, but adiabatic changes in the strength of the trap are experimentally feasible, hence we examine the more general time-dependent case. It should be noted that in the case of a cigar-shaped BEC in which we are interested, a self-consistent reduction of a 3D GP equation to a 1D NLS equation with external potential can be provided by means of a multiple-scale expansion [48] which exploits a small parameter $\delta^2 = (Na_s/a_0)\alpha \ll 1$, where a_s is the s -wave scattering length. The parameter δ indicates the relative strength of the two-body interactions as compared to the kinetic energy of the atoms. In the case we are interested in, in this work, when the finite-size effects along the cigar axes are of primary interest, the same small parameter defines a strong confinement cross section and to the cigar axis by the condition $a_\perp/a_0 \sim \delta\sqrt{\alpha}$. It is important to note, for example, that, for a BEC of $N = 10^4$ of ^{23}Na atoms (with $a_s \approx 2.75$ nm) having characteristic sizes $a_0 = 300 \mu\text{m}$ and $a_\perp = 10 \mu\text{m}$, one gets $\alpha = 0.11$ and $\delta^2 \simeq 0.01$.

In the above mentioned reduction, the rescaled mean-field wave function $u(x,t)$ of the condensate that appears in Eq. (2) is connected to the original order parameter $\Psi(\mathbf{r},t)$ through the relation

$$\Psi(\mathbf{r},t) = \frac{\delta}{a_\perp\sqrt{a_s}} \exp(-i\omega_\perp t) \exp\left(-\frac{\mathbf{r}^2}{2a_\perp^2}\right) u\left(\frac{\delta x}{a_\perp}, \frac{\delta^2\omega_\perp}{2} t\right), \quad (4)$$

where $\mathbf{r} = (y,z)$ and ω_\perp is the harmonic frequency corresponding to the cross section, and physical space and time coordinates (x,t) are used. In Eq. (2), the potential $V(x,t)$ is measured in units of $\hbar^2 a_\perp^2/8m$, while the rescaled mean-field wave function $u(x,t)$ is of order 1: $u(x,t) = \mathcal{O}(1)$. Under the above condition, $g(x,t) = g_0$ in Eq. (2) coincides with the opposite sign of a_s : $g_0 = -\text{sgn}(a_s) \in \{-1, +1\}$. Henceforth, we work, in the case of constant $g(x,t)$, with $g_0 = -\text{sgn}(a_s)$, which illustrates the focusing (+1) or defocusing (-1) nature of the nonlinearity (which represents the attractive or repulsive nature of the interatomic interactions, respectively). In the case of a spatiotemporal two-body interatomic interaction coefficient, in this work we use a first degree polynomial in x with time-dependent coefficients modulated coefficient parameter

$$g(x,t) = x\tilde{g}(t) + \tilde{g}_0(t), \quad (5)$$

where $\tilde{g}(t)$ and $\tilde{g}_0(t)$ are two real functions of time t . When $\tilde{g}(t) \equiv 0$, Eq. (5) gives a time-dependent s -wave scattering length, $g(x,t) = \tilde{g}_0(t)$, which has been used in many works. In the present paper, we concentrate ourselves on the case when $\tilde{g}(t) \neq 0$.

III. MODIFIED GP EQUATION AND MI OF THE CUBIC DERIVATIVE NLS EQUATION WITHOUT EXTERNAL POTENTIAL

In this section, we first apply the phase imprinting technique to reduce the cubic GP equation (2) with external potential (3) into a derivative cubic GP equation. Then we investigate, in absence of external potential, the MI of constant coefficients cubic derivative NLS equation.

A. Phase imprinting technique: Modified GP equation

To introduce the modified GP equation which describes the impact of cubic derivative terms on the condensates, we consider an additional phase imprint on the order parameter $u(x,t)$ to generate a new order parameter $\psi(x,t)$ as [46]

$$u(x,t) = \psi(x,t) \exp[-i\theta(x,t)], \quad (6a)$$

$$\partial\theta/\partial x = -3\beta(t)|\psi|^2, \quad (6b)$$

$$\partial\theta/\partial t = i\beta(t)[\psi\partial\psi^*/\partial x - \psi^*\partial\psi/\partial x] + 9\beta^2(t)|\psi|^4. \quad (6c)$$

Here, $\theta(x,t)$ is a spatiotemporal phase imprint and $\beta(t)$ is a time-dependent real function, and ψ^* stands for the complex conjugate of ψ . Inserting ansatz (6a) into Eq. (2) and using Eqs. (6b)–(6c) yield

$$i\frac{\partial\psi}{\partial t} + \left[\frac{\partial^2}{\partial x^2} + V(x,t) + g(x,t)|\psi|^2\right]\psi + 4i\beta(t)\frac{\partial(\psi^2\psi^*)}{\partial x} = 0. \quad (7)$$

It is important to notice that the last term in Eq. (7) contains two terms, $|\psi|^2\partial\psi^*/\partial x$ and $|\psi|^2\partial\psi/\partial x$; in fact, $\partial(\psi^2\psi^*)/\partial x = \psi^2\partial\psi^*/\partial x + 2|\psi|^2\partial\psi/\partial x$. The spatiotemporal phase imprint $\theta(x,t)$ which arises from Eq. (6b) can be realized experimentally by giving an instantaneous exposure of condensates to electromagnetic fields while the time-dependent phase imprint originates from Eq. (6c) and one has to determine how this can be experimentally implemented [46]. The functional imprint parameter $\beta(t)$ represents the relative magnitudes of the nonlinear dispersion term. When $\alpha(t) = 0$ and $\beta(t) = \beta$ are real constants, Eq. (7) reduces to the well known derivative cubic nonlinear Schrödinger equation, derived in the contexts of binary fluid convection and nonlinear electrical transmission lines [49,50]. It should be noted that transformations (6a)–(6c) do not affect the number N of atoms of the condensate.

It is obvious that Eq. (7) under the condition $\beta(t) = 0$ reduces to the cubic GP Eq. (2) involving two-body interatomic interactions alone and hence we call Eq. (7) the “derivative cubic” or modified GP equation. The last term $4i\beta(t)\frac{\partial(\psi^2\psi^*)}{\partial x}$ in this equation represents the delayed nonlinear response of the system which offsets the modulation generally arising due to three-body interactions. This last term allows the investigation of the MI of BECs described by the GP equation (2) with potential (3) for both focusing and defocusing nonlinearities.

B. MI of constant coefficients cubic derivative NLS equation without external potential

In this section, we investigate the modulational instability of the constant coefficients cubic derivative NLS (7) without external potential:

$$i\frac{\partial\psi}{\partial t} + \left[\frac{\partial^2}{\partial x^2} + g_0|\psi|^2\right]\psi + 4i\beta\frac{\partial\psi^2\psi^*}{\partial x} = 0. \quad (8)$$

It is obvious that for every real constant ϕ_0 and q , the function

$$\psi(x,t) = \phi_0 \exp\{iqx - i[q^2 + (4\beta q - g_0)\phi_0^2]t\} \quad (9)$$

is a constant-amplitude solution of Eq. (8). According to linear stability analysis (LSA), we slightly perturb solution (9) as

follows:

$$\psi(x,t) = [\phi_0 + \varepsilon(x,t)] \exp \{iqx - i[q^2 + (4\beta q - g_0)\phi_0^2]t\}, \quad (10)$$

where $\varepsilon(x,t)$ is a complex function satisfying the condition $|\varepsilon(x,t)| \ll |\phi_0|$, i.e., very small when compared with ϕ_0 . Substituting ansatz (10) into Eq. (8), we obtain the first order approximation

$$i \frac{\partial \varepsilon}{\partial t} + \frac{\partial^2 \varepsilon}{\partial x^2} + 2i(q + 4\beta\phi_0^2) \frac{\partial \varepsilon}{\partial x} + 4i\beta\phi_0^2 \frac{\partial \varepsilon^*}{\partial x} + \phi_0^2(g_0 - 4\beta q)(\varepsilon + \varepsilon^*) = 0. \quad (11)$$

Seeking the perturbation $\varepsilon(x,t)$ in the form

$$\varepsilon = U_1 \exp[i(Qx - \Omega t)] + U_2^* \exp[-i(Qx - \Omega^* t)] \quad (12)$$

and requesting that $|U_1| + |U_2| > 0$, we find the dispersion relation connecting the wave number Q and the frequency Ω of the perturbation to be of the form

$$[\Omega - 2Q(q + 4\beta\phi_0^2)]^2 = Q^2[\phi_0^2(16\beta^2\phi_0^2 + 8q\beta - 2g_0) + Q^2]. \quad (13)$$

It follows from the dispersion relation (13) that the instability region for the cubic derivative NLS, in the absence of an external potential, appears for perturbation wave numbers,

$$Q^2 < 2\phi_0^2(g_0 - 8\beta^2\phi_0^2 - 4q\beta), \quad (14)$$

and, in particular, for both focusing and defocusing nonlinearities with a suitable choice of $\beta = \beta(g_0, q, \phi_0)$. In fact, condition (14) is valid as soon as $\beta \in D_\beta =](-2q - 2\sqrt{q^2 + 2g_0\phi_0^2})/8\phi_0^2, (-2q + 2\sqrt{q^2 + 2g_0\phi_0^2})/8\phi_0^2[$. This assumes that $q^2 + 2g_0\phi_0^2 > 0$, which is satisfied for every real number q and ϕ_0 for focusing nonlinearities ($g_0 = +1$); in

the case of defocusing nonlinearities ($g_0 = -1$), this last inequality is satisfied only for q and ϕ_0 that satisfy the condition $q^2 - 2\phi_0^2 > 0$. Henceforth, we call condition $q^2 + 2g_0\phi_0^2 > 0$ the necessary condition of the MI of the plane-wave solutions of the cubic derivative NLS equation in the absence of external source; any parameter β in the above interval will be called the imprint parameter of the MI. For focusing nonlinearities, the case where $\beta = 0$ has been well investigated in Ref. [18]. From this point onward, we only work with $\beta \neq 0$.

Under condition (14), the growth rate (gain) of modulational instability (for the NLS equation without external potential) is given by the relation

$$|\text{Im } \Omega| = |Q| \sqrt{(2g_0 - 16\beta^2\phi_0^2 - 8q\beta)\phi_0^2 - Q^2}, \quad (15)$$

where β is any imprint parameter of the MI. It is evident that the function $B(\beta) = 2g_0 - 16\beta^2\phi_0^2 - 8q\beta$ reaches its maximal value in D_β at the critical point $\beta_c = -\frac{1}{4}\frac{q}{\phi_0^2}$, which does not depend on g_0 . The presence of the imprint parameter β significantly modifies the instability domain and brings interesting effects. In fact, first it makes possible the investigation of the MI of cubic derivative NLS equation in the case of defocusing nonlinearities ($g_0 = -1$). Second, different values of the imprint parameter β of the MI correspond to different instability diagrams. In Fig. 1, we plot the instability growth rate according to Eq. (15) for different values of β with $\phi_0 = 1$ and $q = 2$. According to this figure, we have two scenarios, depending on whether $\beta \in D_\beta$ is above the critical value ($\beta \geq \beta_c$) or below the critical value ($\beta \leq \beta_c$). In the top panel of Fig. 1 where β is above the critical value ($\beta \geq \beta_c$), we can easily realize that the gain decreases with $|\beta|$, while in the bottom panel where β is below the critical value ($\beta \leq \beta_c$), the gain increases when $|\beta|$ decreases. Thus, the imprint parameter β of the MI, when taken above the critical value

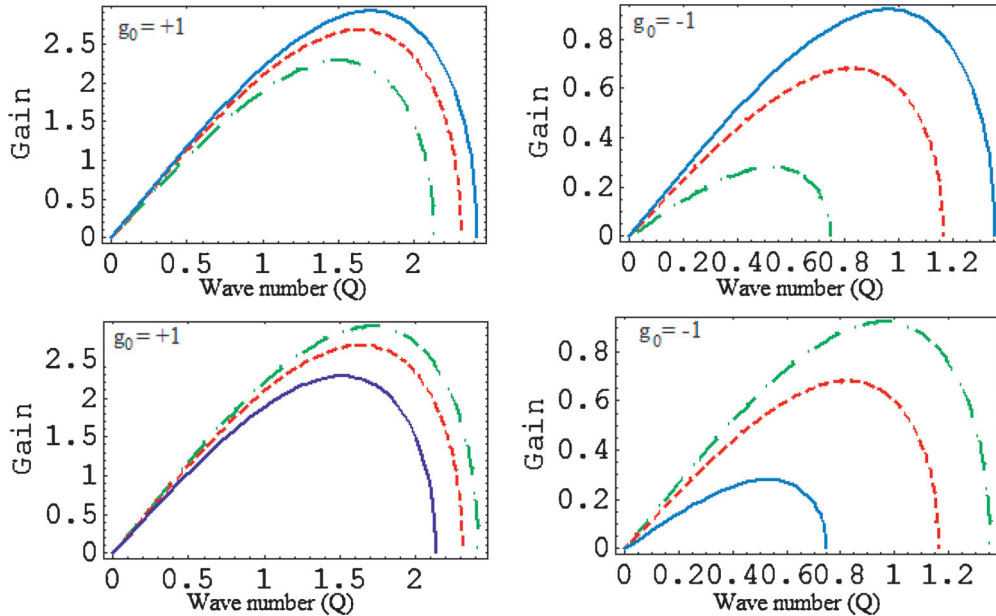


FIG. 1. (Color online) Instability growth rate according to Eq. (15) for three values of the imprint parameter β of the MI with $\phi_0 = 1$ and $q = 2$. The top panel uses three values of $\beta > \beta_c = -0.5$: $\beta = -0.4$ (solid line), -0.3 (dashed line), and -0.2 (dash-dotted line); the bottom panel uses three values of $\beta < \beta_c = -0.5$: $\beta = -0.8$ (solid line), -0.7 (dashed line), and -0.6 (dash-dotted line). The left and the right panels correspond to focusing and defocusing nonlinearities, respectively. All quantities are dimensionless.

β_c softens the instability, and, on the other hand, it relatively enhances the instability when taken below the critical value β_c . Comparing the left panel (focusing nonlinearities) with the right one (defocusing nonlinearities), it appears that the MI is stronger in the case of focusing nonlinearities.

IV. MI OF DERIVATIVE CUBIC NLS EQUATION WITH QUADRATIC EXTERNAL POTENTIAL

The external potential (3) appears as the most physically relevant example of an external potential in the BEC case and gives the harmonic confinement of the atoms by experimentally used magnetic traps [14,47]. The purpose of the present section is to investigate the MI of the modified GP equation (7) via a derivative cubic NLS equation with quadratic external potential that we have derived with the help of a generalized lens transformation.

A. Generalized lens transformation and the derivative cubic NLS equation with external potential

In order to examine the MI related properties in the case when the external potential is present, we first perform a modified lens-type transformation (generalized of lens transformation) of the form

$$\psi(x,t) = \frac{1}{\ell(t)} \phi \exp[if(t)x^2 + \eta(t)]. \quad (16)$$

Here, $T = T(t)$, $\ell(t)$ and $f(t)$ are three time-dependent real functions, and $X(x,t) = x\ell^{-1}(t)$ is a spatiotemporal real function. This kind of transformation has been used for deriving atomic solitons of Bose–Einstein condensates consisting of sodium and rubidium atoms when one starts from the known optical soliton solution of the NLS equation in the absence of external potential [51]. To preserve the scaling, we follow Refs. [52,53] and choose

$$\frac{dT}{dt} = \frac{1}{\ell^2(t)}. \quad (17)$$

By inserting (16) into Eq. (7) and taking expressions (5) for $g(x,t)$ and (17) into account, the resulting equations can be satisfied if

$$\frac{df}{dt} + 4f^2 + \alpha = 0, \quad (18a)$$

$$\frac{d\ell}{dt} - 4f(t)\ell = 0, \quad (18b)$$

$$\frac{d\eta}{dt} + 2f(t) - \frac{1}{\ell} \frac{d\ell}{dt} = 0, \quad (18c)$$

$$\beta(t) = \tilde{g}(t)f^{-1}(t)/8. \quad (18d)$$

Solving Eqs. (18b) and (18c) in terms of $f(t)$ yields

$$\ell(t) = \ell(0) \exp\left(4 \int_0^t f(s) ds\right), \quad (19a)$$

$$\eta(t) = 2 \int_0^t f(s) ds + \eta(0). \quad (19b)$$

The problem of finding the time dependence of the parameters $T(t)$ and $\ell(t)$ is then reduced to the solution of Riccati equation (18a). To solve Eq. (18a), one needs a particular

solution with the help of which the equation can be transformed into Bernoulli equation.

Under conditions (17)–(18d), the equation for $\phi(X,T)$ becomes

$$i \frac{\partial \phi}{\partial T} + \frac{\partial^2 \phi}{\partial X^2} + \lambda_0 |\phi|^2 \phi + i\lambda \frac{\partial(\phi^2 \phi^*)}{\partial X} = 0, \quad (20)$$

where

$$\lambda_0 = \tilde{g}_0(t) \exp[2\eta(t)], \quad \lambda = 4 \frac{\beta(t)}{\ell(t)} \exp[2\eta(t)]. \quad (21)$$

Generally, λ_0 and λ are real and depend on the time t . Thus, we retrieve the cubic derivative NLS equation with time-dependent coefficients. It is important to notice from ansatz (16) that $\eta(t)$ influences the number of atoms N in the condensate. In fact, using the phase imprint ansatz (6a)–(6c) and the lens transformation (16) we have $N = \int_{\mathbf{R}} |u|^2 dx = \exp[\eta(t)] \int_{\mathbf{R}} |\phi|^2 dX$. According to Eq. (19b), $\exp[\eta(t)] = \exp[2 \int_0^t f(s) ds + \eta(0)]$, which means that the number of atoms in the condensate grows exponentially if $f(t)$, solution of the Riccati equation (18a), is positive, and will decrease exponentially if $f(t)$ is negative. We can then conclude that a positive $f(t)$ is associated with the feeding of atoms in the condensate, while the negative $f(t)$ corresponds to the loss of atoms in the condensate. It is obvious that the function $f(t)$ depends on the strength of the magnetic trap $\alpha(t)$, while its sign is independent of that of $\alpha(t)$. For example, if $\alpha(t) = -\alpha_0^4$ is a negative constant (which corresponds to a confining potential), then $f(t) = \pm\alpha_0^2/2$ will be two particular solutions of the Riccati equation (18a). If working in the presence of feeding (loss) of atoms in the condensate, one may then work with positive (negative) $f(t)$.

B. Investigation of the MI for the derivative cubic NLS equation

In this subsection, we investigate the MI for the cubic derivative NLS equation (20). We start with the derivation of the analytical expression of the dispersion relation which is appropriate for investigating the MI of constant amplitude wave solution of Eq. (20). Then, we separately analyze the cases of derivative cubic NLS equation (20) with constant coefficients and with distributed coefficients.

1. Linear stability analysis and criterion of the MI for the cubic derivative NLS

To investigate the MI for the cubic derivative NLS equation (20), we follow the LSA technique and look for an ansatz in the form

$$\phi = [\phi_0 + \varepsilon] \exp\left[-iQX - i \int_0^T \Omega(\nu) d\nu\right], \quad (22)$$

where $\Omega(T)$ is a real time-dependent function representing the nonlinear frequency shift, ϕ_0 is a real constant, Q is the wave number of the carrier, and $\varepsilon(X,T)$ is a small perturbation of the wave amplitude ($|\varepsilon| \ll 1$). Substituting ansatz (22) into Eq. (20) and linearizing $\delta\phi$ and its complex conjugate ε^* , we obtain, after taking

$$\Omega(T) = Q^2 - \lambda_0(t)\phi_0^2 - Q\phi_0^2\lambda(t), \quad (23)$$

that ε satisfies the linear equation

$$i \frac{\partial \varepsilon}{\partial T} + \frac{\partial^2 \varepsilon}{\partial X^2} + 2i(\lambda \phi_0^2 - Q) \frac{\partial \varepsilon}{\partial X} + i\lambda \phi_0^2 \frac{\partial \varepsilon^*}{\partial X} + \phi_0^2(\lambda_0 + \lambda Q)(\varepsilon + \varepsilon^*). \quad (24)$$

Let us seek the perturbation $\varepsilon(X, T)$ in the form

$$\varepsilon = U_1 \exp\left(iKX - i \int_0^T \omega(v) dv\right) + U_2^* \exp\left(-iKX + i \int_0^T \omega^*(v) dv\right), \quad (25)$$

where $KX - \int_0^T \omega(v) dv$ is the modulation phase in which K and ω are the wave number and the complex frequency of the modulation waves, respectively, and U_1 and U_2 are two complex numbers. The MI may set in provided the complex frequency ω has a non-null imaginary part. Inserting Eq. (25) into Eq. (24) and requesting that $|U_1| + |U_2| > 0$ yield the time-dependent dispersion relation

$$[\omega - 2K(\lambda \phi_0^2 - Q)]^2 - K^2 [K^2 + \phi_0^2(\lambda^2 \phi_0^2 - 2Q\lambda - 2\lambda_0)] = 0. \quad (26)$$

For ω to have a non-null imaginary part, it is necessary and sufficient that

$$K^2 + \phi_0^2(\lambda^2 \phi_0^2 - 2Q\lambda - 2\lambda_0) < 0. \quad (27)$$

Inequality (27) is the criterion of the MI for the cubic derivative NLS equation (20). Under the MI criterion (27), the local growth rate (gain) of modulational instability is given by the relation

$$|\text{Im} \omega(t)| = |K| \sqrt{\phi_0^2 [2Q\lambda(t) + 2\lambda_0(t) - \lambda^2(t)\phi_0^2] - K^2}. \quad (28)$$

2. MI for the derivative cubic NLS equation with constant coefficients

A particularly simple and interesting case is when λ_0 and λ are constants. Then from system (17)–(18d), it follows that $\beta(t)$ must be a constant and $\tilde{g}_0(t)$ must satisfy the nonlinear second order ordinary differential equation

$$y \frac{d^2 y}{dt^2} - 2 \left(\frac{dy}{dt} \right)^2 - 4\alpha(t)y^2 = 0. \quad (29)$$

In the case of constant λ_0 and λ , the problem of finding the time dependence of the parameters then reduces to solve Eq. (29). The simplest way to work with Eq. (29) is to solve it for $\alpha(t)$ when $\tilde{g}_0(t)$ is known. For example, any $\tilde{g}_0(t) = \tilde{a}_0 \exp(\tilde{\lambda}t)$ (see Ref. [46]) corresponds to constant $\alpha(t) = -\tilde{\lambda}^2/4$.

As it is indicated in Ref. [18], one of the most interesting cases in the setting with the harmonic potential is the one with the inverse square dependence (of the trap amplitude, for a given x) on time of equation

$$\alpha(t) = A(t + t^*)^{-2}, \quad (30)$$

for an arbitrary nonzero real constant A . Inserting Eq. (30) into Eq. (29) yields

$$\tilde{g}_0(t) = \frac{4\lambda_0\beta}{\lambda\ell(0)} \left(\frac{t + t^*}{t^*} \right)^m, \quad m = \frac{-1 \pm \sqrt{1 - 16A}}{2}. \quad (31)$$

For $\tilde{g}_0(t)$ to be a real function of time t , the parameter A of the strength of the magnetic trap $\alpha(t)$ must satisfy the condition $A < 1/16$. This condition on A allows us to investigate the MI of the cubic derivative NLS equation for both confining potential ($A < 0$) and repulsive potential ($A > 0$). In Eq. (30), t^* is an arbitrary constant which essentially determines the “width” of the trap at time $t = 0$. It is important to notice that $t^* < 0$ describes a BEC in a shrinking trap, while the case $t^* > 0$ corresponds to a broadening condensate. Inserting Eq. (30) into system (18a)–(18d), all the time-dependent parameters are explicitly defined; in particular, we have $T(t) = t^* (2m + 1)^{-1} \ell^{-2}(0) [(t+t^*)^{2m+1} - 1]$. To guarantee the variation of T from zero to infinity, we must take $m = (-1 + \sqrt{1 - 16A})/2$ in the case of broadening condensates, and $m = (-1 - \sqrt{1 - 16A})/2$ for BECs in a shrinking trap. In the latter case, we focus our study on the case where t goes from zero to $-t^*$; this avoids a singularity at $t = -t^*$ and guarantees the variation of T from zero to $+\infty$.

In the case of constant λ_0 and λ , the growth rate (gain) of modulational instability is time independent, but depends on the imprint parameter β :

$$|\text{Im} \omega(\beta)| = |K| \sqrt{\phi_0^2 [-\lambda^2(\beta)\phi_0^2 + 2Q\lambda(\beta) + 2\lambda_0] - K^2}. \quad (32)$$

It is evident that the variation of the growth rate, related to the imprint parameter β , may significantly modify the instability domain and bring interesting effects. In fact, to different values β correspond different instability diagrams, depending on whether $\lambda = \lambda(\beta)$ is positive or negative. Negative $\lambda(\beta)$ softens the instability, while positive one [$\lambda(\beta) > 0$] relatively enhances the instability. This behavior is shown in Fig. 2 through the MI gain provided by Eq. (32), as a function of the perturbation wave number K , for three values of negative $\lambda(\beta)$ [Fig. 2(a)] and three values of positive $\lambda(\beta)$ [Fig. 2(b)]. In Fig. 2(a), obtained with negative $\lambda(\beta)$, it is easily seen that the gain decreases with the imprint parameter λ , while in Fig. 2(b) with positive $\lambda(\beta)$, the gain increases when the imprint parameter λ increases.

We can summarize the result for constant λ_0 and λ as follows. For the MI of constant amplitude plane-wave solutions $\phi = \phi_0 \exp(-iQX - i[Q^2 - \lambda_0\phi_0^2 - Q\phi_0^2\lambda]T)$, it is necessary and sufficient that the wave number K of the modulation waves satisfies the MI criterion (27). Moreover, for given ϕ_0 , Q , and λ_0 , the imprint parameter β should be chosen such that $\lambda^2(\beta)\phi_0^2 - 2Q\lambda(\beta) - 2\lambda_0 < 0$.

3. MI for the derivative cubic NLS equation with time-dependent coefficients

Let us now look at the case when at least one of λ_0 and λ is not constant. As in the previous case, if we consider the harmonic potential with the inverse square dependence on the time trap amplitude (30) with $A < 1/16$, we found as a

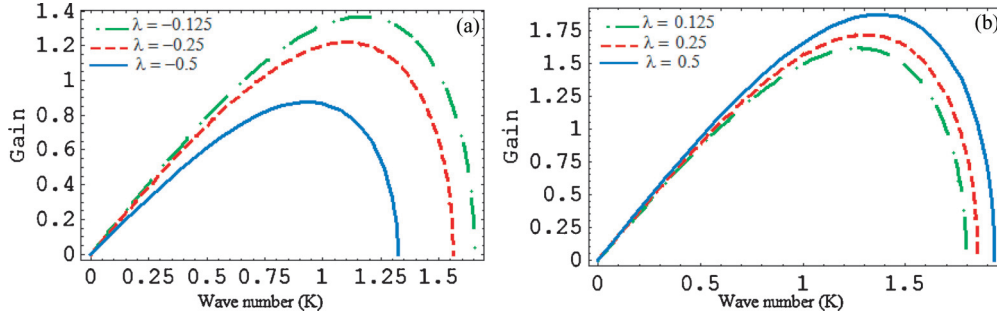


FIG. 2. (Color online) Instability growth rate according to Eq. (32) for three positive values and three negative values of the imprint parameter $\lambda(\beta)$. (a) Case of negative values of $\lambda(\beta)$ with $\lambda(\beta) = -0.125, -0.25,$ and -0.50 . (b) Case of positive values of $\lambda(\beta)$ with $\lambda(\beta) = 0.125, 0.25,$ and 0.50 . The other parameters are $Q = 1, \phi_0 = 1,$ and $\lambda_0 = 3/2$.

particular solution of Riccati equation (18a)

$$f(t) = B(t + t^*)^{-1}, \quad B = \frac{1 \pm \sqrt{1 - 16A}}{8}. \quad (33)$$

With the help of the particular solution (33), the general solution of Eq. (18a) reads

$$f(t) = \frac{1 - 4B + CB(1 - 8B)(t + t^*)^{8B-1}}{C(1 - 8B)(t + t^*)^{8B} + 4(t + t^*)}, \quad (34)$$

where $C = \frac{1 - 4B - 4f(0)t^*}{[f(0)(1 - 8B)(t^*)^{8B} - B(1 - 8B)(t^*)^{8B-1}]}$. Using (30) and (33), we obtain the time dependence of the following parameters:

$$\ell(t) = \ell(0) \left(\frac{t + t^*}{t^*} \right)^{4B}, \quad (35a)$$

$$\eta(t) = 2B \ln \left| \frac{t + t^*}{t^*} \right| + \eta(0), \quad (35b)$$

$$\beta(t) = \frac{\tilde{g}(t)(t + t^*)}{8B}, \quad (35c)$$

$$T(t) = \frac{1}{\ell(0)(1 - 4B)} \left[(t + t^*) \left(\frac{t^*}{t + t^*} \right)^{4B} - t^* \right]. \quad (35d)$$

It follows from system (35a)–(35d) that $\beta(t)$ is no longer a functional parameter, but depends of $\tilde{g}(t)$. In the case of positive t^* (broadening condensate), it is reasonable to take B such that $1 - 4B$ should be positive; a proper choice of $\ell(0)$ will then ensure a variation of $T(t)$ from zero to $+\infty$. For BECs in a shrinking trap ($t^* < 0$), a good choice of $\ell(0)$ and

$B > 1/4$ and working with $0 \leq t < t^*$ will avoid singularity at t^* and ensure a variation of $T(t)$ from zero to $+\infty$.

In the case at least one of λ_0 and λ is not constant, the growth rate (gain) of modulational instability (28) is time dependent. In this case, the variation of the growth rate, related to the sign of t^* , i.e., on whether t^* describes a BEC in a shrinking trap ($t^* < 0$) or corresponds to a broadening condensate, may significantly affect the instability domain and bring new effects. Indeed, to different signs of t^* correspond different instability diagrams. Negative t^* relatively enhances the instability, while positive t^* softens the instability. This behavior is shown in Fig. 3 through the MI gain provided by Eq. (28), as a function of the perturbation wave number K , for three negative values of t^* [plot (a)] and three positive values of t^* [plot (b)]. In Fig. 3(a) corresponding to BECs in a shrinking trap ($t^* < 0$), one easily realizes that the gain increases with t^* , while in Fig. 3(b) obtained for broadening condensates ($t^* > 0$), the gain decreases as t^* increases. The plots in this figure are obtained with $\tilde{g}_0(t) = 2 \exp(0.5t)$ and $\tilde{g}(t) = 2 \exp(-t)$.

From our analysis, it is clear that the simplest and most interesting case in the setting with a time-dependent harmonic potential is the one with the inverse square dependence (of the trap amplitude, for a given x) on time of Eq. (30) with $A < 1/16$. In this case, the modified lens transformation suggests the equivalence with a cubic derivative NLS equation. In this special case of interest, the coefficients of the cubic derivative NLS equation are either constant or time dependent, suggesting that the frequencies of the modulation waves are either constant or time dependent.

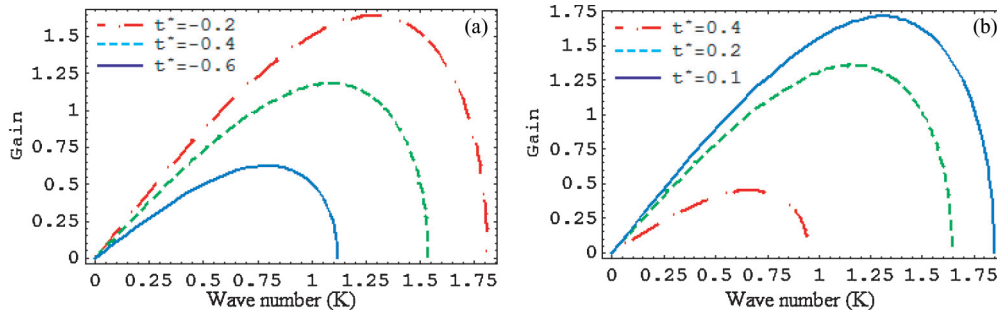


FIG. 3. (Color online) Instability growth rate according to Eq. (28) for three positive values and three negative values t^* at time $t = 0$. (a) Case of BECs in a shrinking trap ($t^* < 0$) with $t^* = -0.6, -0.4,$ and -0.2 . (b) Case corresponding to broadening condensates ($t^* > 0$) with $t^* = 0.1, 0.2,$ and 0.4 . The other parameters are $Q = 1, \phi_0 = 1, A = -1, \ell(0) = 1, \eta(0) = 0, \tilde{g}_0(t) = 2 \exp(0.5t), \tilde{g}(t) = 2 \exp(-t), B = (1 + \sqrt{17})/8$ for plot (a) and $B = (1 - \sqrt{17})/8$ for plot (b).

V. SOLITARY-WAVE SOLUTIONS OF THE EFFECTIVE 1D GP EQ. (2) WITH SPATIOTEMPORAL POTENTIAL (3)

Due to the suggested analogy with a cubic derivative NLS with a constant coefficient gain where the modulational stability analysis has been completely performed, the most interesting case of the spatiotemporal potential (3) is the case of $\alpha(t) = A(t + t^*)^{-2}$ with $A < 1/16$, which we now investigate analytically. We limit ourselves to constant λ_0 and λ in Eq. (20) and apply the F expansion method to find a large class of solitary-wave solutions.

We are mainly interested in analytical solitary-wave solutions of constant coefficients derivative cubic NLS equation (20). Conditions that $\beta(t)$ should be a constant and $\tilde{g}_0(t)$ should be a solution of Eq. (29) are the integrability condition of Eq. (2). In order to find a large class of solitary-wave solution, the F -expansion technique is used.

In order to find a large class of solitary-wave solution of Eq. (20) with constant coefficients, we perturb the Stokes wave solution $\phi(X, T) = \phi_0 \exp[-ik_0 X + i(\lambda_0 \phi_0^2 + k_0 \lambda \phi_0^2 - k_0^2) T]$ of Eq. (20) to obtain its solitary-wave solutions. Writing a solution of Eq. (20) in polar form,

$$\phi(X, T) = R(X, T) \exp[i\Phi(X, T)], \quad (36)$$

we obtain the following system for the definition of the real functions $R(X, T)$ and $\Phi(X, T)$:

$$\begin{aligned} -R\partial\Phi/\partial T + \partial^2 R/\partial X^2 - R(\partial\Phi/\partial X)^2 \\ - \lambda R^3 \partial\Phi/\partial X + \lambda_0 R^3 &= 0, \\ \partial R/\partial T + 2(\partial\Phi/\partial X)(\partial R/\partial X) \\ + R\partial^2\Phi/\partial X^2 + 3\lambda R^2\partial R/\partial X &= 0. \end{aligned} \quad (37)$$

Now, we use the above Stokes solution to perturb system (37) as follows:

$$\begin{aligned} R(X, T) &= \phi_0 + \rho(z = X - \nu T), \\ \Phi(X, T) &= -k_0 z + \varphi(z) + (\lambda_0 \phi_0^2 + \lambda k_0 \phi_0^2 - k_0^2 - k_0 \nu) T, \end{aligned} \quad (38)$$

ν being an arbitrary constant (traveling wave velocity). Inserting (38) into (37) and integrating the resulting second equation yield

$$\frac{d\varphi}{dz} = \frac{C_0}{(\phi_0 + \rho)^2} + \frac{(\nu + 2k_0)}{2} - \frac{3\lambda}{4}(\phi_0 + \rho)^2, \quad (39)$$

where C_0 is a constant of integration. Inserting the expression for $\frac{d\varphi}{dz}$ into the first resulting equation yields

$$\left(\frac{d\zeta}{dz}\right)^2 = \tilde{\alpha}\zeta^4 + 4\tilde{\beta}\zeta^3 + 6\tilde{\gamma}\zeta^2 + 4\tilde{\delta}\zeta + \tilde{\epsilon} = f(\zeta), \quad (40)$$

where

$$\begin{aligned} \zeta(z) &= [\phi_0 + \rho(z)]^2, \\ \tilde{\alpha} &= -\lambda^2, \\ \tilde{\beta} &= (\lambda\nu - 2\lambda_0)/4, \\ \tilde{\gamma} &= [4\lambda_0\phi_0^2 + 2\lambda(2k_0\phi_0^2 - C_0) - 4\nu k_0 - \nu^2 - 4k_0^2]/6, \\ \tilde{\delta} &= \text{const}, \\ \tilde{\epsilon} &= -4C_0^2. \end{aligned} \quad (41)$$

It is important to notice that $\tilde{\delta}$ and C_0 are two arbitrary real constants (constants of integration).

It is known since 1865 (see Ref. [54], p. 454) that solutions to Eq. (40) are given in terms of Weierstrass' elliptic function $\wp(z; g_2, g_3)$ (see Ref. [55], pp. 4–16) by

$$\zeta(z) = \zeta_0 + \frac{\sqrt{f'(\zeta_0)} \frac{d\wp(z; g_2, g_3)}{dz} + \frac{f'(\zeta_0)}{2} [\wp(z; g_2, g_3) - \frac{1}{24} f''(\zeta_0)] + \frac{1}{24} f(\zeta_0) f'''(\zeta_0)}{2 [\wp(z; g_2, g_3) - \frac{1}{24} f''(\zeta_0)]^2 - \frac{1}{48} f(\zeta_0) f^{(IV)}(\zeta_0)}, \quad (42)$$

where ζ_0 is an arbitrary real constant, not necessarily a zero of the polynomial $f(\zeta)$ and $f' = df/d\zeta$. The invariants g_2 and g_3 of the function $\wp(z; g_2, g_3)$ are related to the coefficients of $f(\zeta)$ according to Ref. [54]

$$\begin{aligned} g_2 &= \tilde{\alpha}\tilde{\epsilon} - 4\tilde{\beta}\tilde{\delta} + 3\tilde{\gamma}^2, \\ g_3 &= \tilde{\alpha}\tilde{\gamma}\tilde{\epsilon} + 2\tilde{\beta}\tilde{\gamma}\tilde{\delta} - \tilde{\alpha}\tilde{\delta}^2 - \tilde{\gamma}^3 - \tilde{\epsilon}\tilde{\beta}^2. \end{aligned} \quad (43)$$

The so-called discriminant Δ of Weierstrass' elliptic function $\wp(z; g_2, g_3)$ (see Ref. [56], p. 44)

$$\Delta = g_2^3 - 27g_3^2 \quad (44)$$

is suitable to classify the behavior of the solution $\zeta(z)$ and to discriminate between periodic and solitary-wave-like solutions [55]. If $\Delta = 0$, $g_2 \geq 0$, and $g_3 \leq 0$, $\zeta(z)$ is solitary-wave-like and is given by

$$\zeta(z) = \zeta_0 + \frac{f'(\zeta_0)}{4 \left[e_1 - \frac{1}{24} f''(\zeta_0) + 3e_1 \text{cosech}^2(\sqrt{3e_1} z) \right]}, \quad (45a)$$

if $e_1 > 0$,

$$\zeta(z) = \zeta_0 + \frac{f'(\zeta_0) z^2}{4 \left[1 - \frac{f''(\zeta_0)}{24} z^2 \right]}, \quad \text{if } e_1 = 0, \quad (45b)$$

where $e_1 = \sqrt[3]{-g_3}$. Because $\tilde{\delta}$ and C_0 are two arbitrary constants of integration, we can, for simplicity, choose $\tilde{\delta}$ and C_0 so that either $\tilde{\delta} = \tilde{\epsilon} = 0$ or $\tilde{\delta} \neq 0$, $\tilde{\epsilon} < 0$ and $g_2 = g_3 = 0$. In both cases, we have $g_2 \geq 0$, $g_3 \leq 0$, and $\Delta = 0$. Then Eq. (45a) defines solitary-wave-like solutions if and only if $\tilde{\gamma} > 0$ and $2\tilde{\beta}^2 - 3\tilde{\alpha}\tilde{\gamma} \geq 0$, while Eq. (45b) describes the intensity of the algebraic solitary waves if $f''(\zeta_0) < 0$. According to the definition of $\zeta(z)$ by system (41), the physical solution (45a) must be non-negative. It is important to mention that a solution $\zeta(z)$ given by Eq. (45a) is said to be physical if it is real and bounded. Considering the phase diagram of $f(\zeta)$, Refs. [57–60], one obtains conditions, expressed in terms of the coefficients of the basic equation, that determine physical solutions [see Fig. 4, obtained from Refs. [57–59] and showing the phase diagrams associated to real and bounded solutions if either $\tilde{\delta} = \tilde{\epsilon} = 0$ (left plots) or $g_2 = g_3 = 0$ (right plots)]. It is important to notice that physical solutions that are obtained

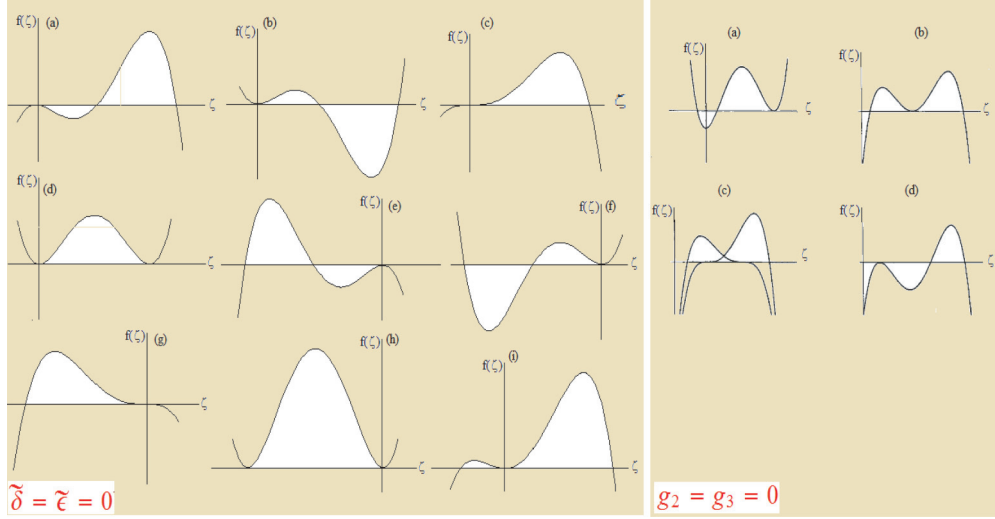


FIG. 4. (Color online) Phase diagrams associated to real and bounded solutions when either $\tilde{\delta} = \tilde{\epsilon} = 0$ or $\tilde{\delta} \neq 0$, $\tilde{\epsilon} < 0$, and $g_2 = g_3 = 0$ (for more explanation, cf. Refs. [57] for the right plots and [59] for left plots).

from the phase diagrams are just possible solutions for our problem. In fact, the solitary-wave solutions that are in our interest must be both physical and non-negative. Thus, we are interested only in non-negative physical solutions. In what follows, we give examples of solitary-wave solutions when either $\tilde{\delta} = \tilde{\epsilon} = 0$ or $\tilde{\delta} \neq 0$, $\tilde{\epsilon} < 0$, and $g_2 = g_3 = 0$.

A. Examples of solitary-wave solutions under conditions $\tilde{\delta} = \tilde{\epsilon} = 0$

According to Ref. [59], we have the following physical solitary-wave-like solutions when $\tilde{\delta} = \tilde{\epsilon} = 0$:

$$\zeta_{\pm}(z) = \frac{\tilde{\gamma}[2\tilde{\beta} \pm \sqrt{4\tilde{\beta}^2 - 6\tilde{\alpha}\tilde{\gamma}}][3\tilde{\gamma}^2 + (\tilde{\gamma}^2 - 1)\cosh^2(\sqrt{\frac{3}{2}}\tilde{\gamma}^3 z)]}{[-3\tilde{\alpha}\tilde{\gamma}^3 + (4\tilde{\beta}^2 \pm 2\sqrt{4\tilde{\beta}^2 - 6\tilde{\alpha}\tilde{\gamma}} - \tilde{\alpha}\tilde{\gamma}(5 + \tilde{\gamma}^2))\cosh^2(\sqrt{\frac{3}{2}}\tilde{\gamma}^3 z)]}. \quad (46)$$

Solutions (46) correspond to the two simple roots of the polynomial $f(\zeta)$ (of course, when $4\tilde{\beta}^2 - 6\tilde{\alpha}\tilde{\gamma} > 0$) and are represented by the phase diagrams (b)–(d) and (f)–(h) in Fig. 4 (for more details, see Ref. [59]).

Let us now investigate the conditions of non-negativity of solutions (46). Here, we distinguish two cases, namely, the case when $\tilde{\gamma} = 1$ and the case when $0 < \tilde{\gamma} \neq 1$. It is obvious that case $\tilde{\gamma} = 1$ is associated only to the bright solitary-wave solution.

(A) If $\tilde{\gamma} = 1$, solutions (46) will be non-negative if and only if $\tilde{\alpha}(2\tilde{\beta}^2 \pm \sqrt{4\tilde{\beta}^2 - 6\tilde{\alpha}} - 18\tilde{\alpha})^{-1} < 2/3$ and $(2\tilde{\beta} \pm \sqrt{4\tilde{\beta}^2 - 6\tilde{\alpha}})(2\tilde{\beta}^2 \pm \sqrt{4\tilde{\beta}^2 - 6\tilde{\alpha}} - 18\tilde{\alpha}) > 0$.

An example of bright solitary-wave-like solution is obtained with the parameters $\lambda_0 = 1$, $\phi_0 = 1$, $\nu = 0.5$, $k_0 = 1$, and $\lambda = 8.25/4$. With this set of parameters, $\zeta_+(z)$ satisfies all the needed conditions (real, bounded, and non-negative). Figures 5–7, respectively, show the effect of t^* , A , and β on the density $|u(x, t)|^2$ at $x = 3$ of the wave function $u(x, t)$ associated with bright solitary-wave-like solutions; here, we used $\ell(0) = 1$. For these three figures, the plots of the left and right panels correspond, respectively, to broadening condensates ($t^* > 0$) and BECs in a shrinking trap ($t^* < 0$), while the plots of the top and bottom panels correspond to confining potential

($A < 0$) and repulsive potential ($A > 0$), respectively. For $x = 3$, Fig. 5 shows the time evolution of the density $|u(x, t)|^2$ for three different values of t^* . As it is easily seen from this figure, the density amplitude in the case of confining potential decreases as t^* increases for broadening condensates, but increases with t^* for BECs in a shrinking trap. In the case of repulsive potential, the density amplitude increases with t^* for both broadening condensates and BECs in a shrinking trap. Figure 6 depicts the density $|u(x, t)|^2$ at $x = 3$ for three different values of A . The plots of this figure show that for both confining potential (top plots) and repulsive potential (bottom plots), the amplitude of the density decreases as A increases; this happens for both broadening condensates (left plots) and BECs in a shrinking trap (right plots). It is seen from the plots in Fig. 7 where the density $|u(x, t)|^2$ at $x = 3$ is depicted for different values of β that independently of the sign of A (confining potential or repulsive potential) and of the sign of t^* (broadening condensates or BECs in a shrinking trap), the wave amplitude decreases as the imprint parameter β increases.

(B) If $0 < \tilde{\gamma} \neq 1$, then solutions (46) will be non-negative if and only if the following three conditions are simultaneously satisfied: (i) $3\tilde{\gamma}^2(1 - \tilde{\gamma}^2)^{-1} \leq 1$, (ii) $3\tilde{\alpha}\tilde{\gamma}^3(4\tilde{\beta}^2 \pm 2\sqrt{4\tilde{\beta}^2 - 6\tilde{\alpha}\tilde{\gamma}} - \tilde{\alpha}\tilde{\gamma}(5 + \tilde{\gamma}^2))^{-1} < 1$, and

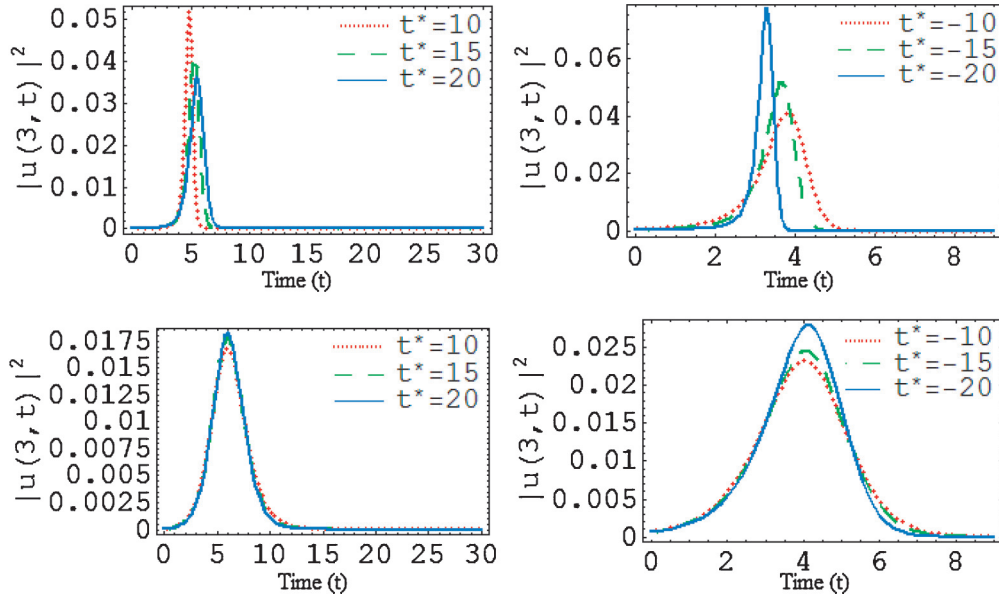


FIG. 5. (Color online) Plots of density $|u(x,t)|^2$ at $x = 3$ (in units of a_{\perp}) for three values of the parameter t^* appearing in potential (30) and showing the effect of t^* on the amplitude of the density. The top and bottom panels correspond to confining potential (with $A = -2$) and repulsive potential (with $A = 1/17$), respectively, while the left and right panels are associated with broadening condensates and BECs in a shrinking trap, respectively. Typical values of all other parameters are given in the text.

(iii) $\tilde{\gamma}(\tilde{\gamma}^2 - 1)(2\tilde{\beta} \pm \sqrt{4\tilde{\beta}^2 - 6\tilde{\alpha}\tilde{\gamma}})(4\tilde{\beta}^2 - \tilde{\alpha}\tilde{\gamma}(5 + \tilde{\gamma}))^2 \pm 2\sqrt{4\tilde{\beta}^2 - 6\tilde{\alpha}\tilde{\gamma}} > 0$. With the parameters $\lambda_0 = 1$, $\phi_0 = 1$, $\nu = 0.5$, $\lambda = 14.25/4$, and $k_0 = 1$, conditions (i)–(iii) are simultaneously satisfied for $\zeta_+(z)$, and hence we have an example of the solitary-wave-like solution from Eq. (40) when $0 < \tilde{\gamma} \neq 1$. With the use of this set of parameters, we depicted in Figs. 8–10, respectively, the density $|u(x,t)|^2$ at $t = 4$ of the wave function $u(x,t)$ associated with the solitary-wave-like solutions (46); Figs. 8–10, respectively,

show the effect of t^* , A , and β on the solitary-wave evolution. Here, we used $\ell(0) = 1$. These three figures have the same disposition as Figs. 5–7: the plots of the left and right panels correspond to broadening condensates ($t^* > 0$) and BECs in a shrinking trap ($t^* < 0$), respectively, while the plots of the top and bottom panels correspond to confining potential ($A < 0$) and repulsive potential ($A > 0$), respectively. Figure 8 shows at time $t = 4$ the spatial evolution of the density $|u(x,t)|^2$ for three different values of t^* . As is easily seen from this

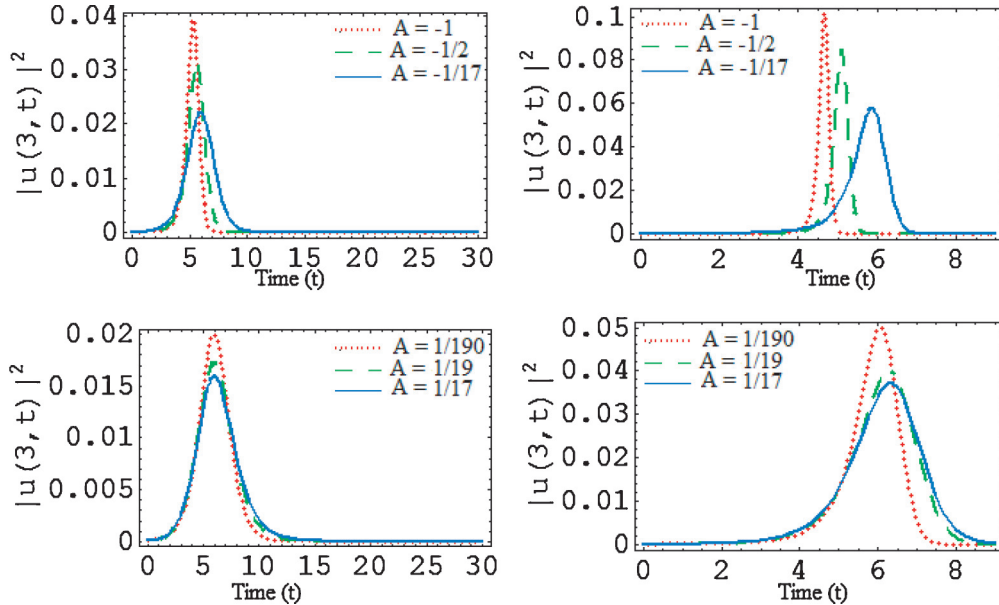


FIG. 6. (Color online) Plots of density $|u(x,t)|^2$ at $x = 3$ (in units of a_{\perp}) for three values of the parameter A appearing in potential (30), showing the effect of A on the amplitude of the density. The top and bottom panels correspond to confining potential and repulsive potential, respectively, while the left and right panels are associated with broadening condensates (with $t^* = 10$) and BECs in a shrinking trap (with $t^* = -10$), respectively. Typical values of all other parameters are given in the text.

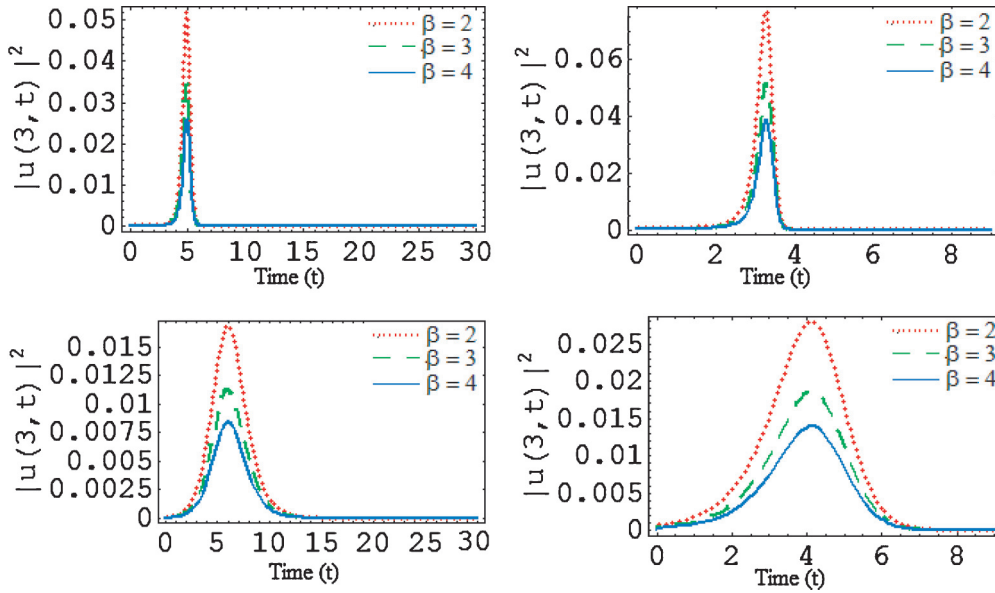


FIG. 7. (Color online) Plots of density $|u(x,t)|^2$ at $x = 3$ (in units of a_{\perp}) for three values of the imprint parameter β appearing in transformation (6b), showing the effect of β on the peak density. The top and bottom panels correspond to confining potential (with $A = -2$) and repulsive potential (with $A = 1/17$), respectively, while the left and right panels are associated with broadening condensates (with $t^* = 10$) and BECs in a shrinking trap (with $t^* = -10$), respectively. Typical values of all other parameters are given in the text.

figure, the peak density in the case of confining potential decreases as t^* increases for broadening condensates (top panels), but increases with t^* for BECs in a shrinking trap. In the case of repulsive potential (bottom panels), the peak density increases with t^* for both broadening condensates and BECs in a shrinking trap. Figure 9 depicts the density $|u(x,t)|^2$ at time $t = 4$ for three different values of A . The plots of this figure show that for both the confining potential (top plots) and the repulsive potential (bottom plots), the

peak density decreases as A increases; this happens for both broadening condensates (left plots) and BECs in a shrinking trap (right plots). It is seen from the plots in Fig. 10 where the density $|u(x,t)|^2$ at time $t = 4$ is depicted for different values of β that, independently of the sign of A (confining potential or repulsive potential) and of the sign of t^* (broadening condensates or BECs in a shrinking trap), the peak density decreases as the imprint parameter β increases.

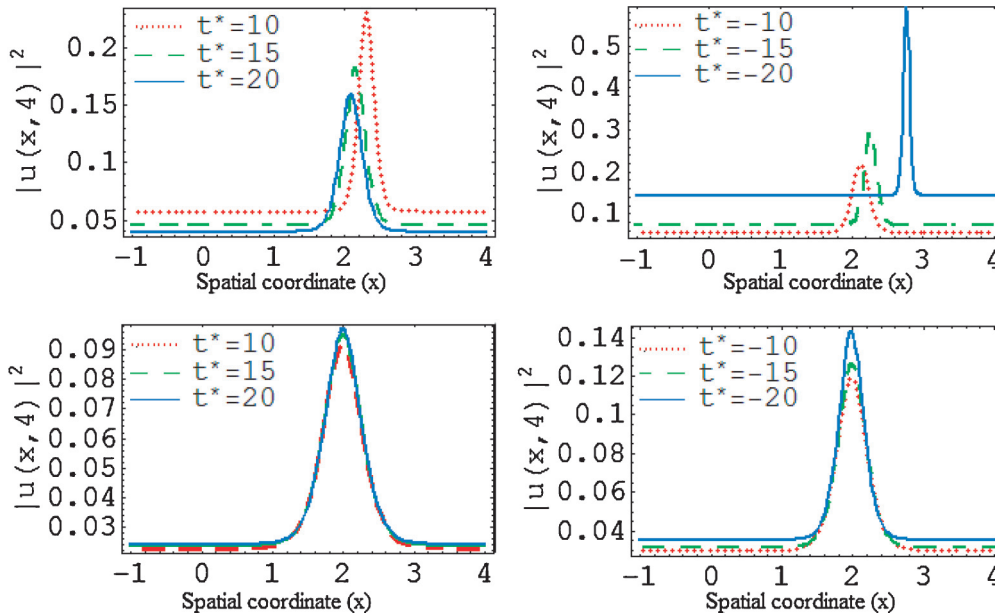


FIG. 8. (Color online) Density $|u(x,t)|^2$ at time $t = 4$ (in units of $2/\omega_{\perp}$) for three values of the parameter t^* appearing in potential (30), showing the effect of t^* on the peak density. The top and bottom panels correspond to confining potential (with $A = -2$) and repulsive potential (with $A = 1/17$), respectively, while the left and right panels are associated with broadening condensates and BECs in a shrinking trap, respectively. Typical values of all other parameters are given in the text.

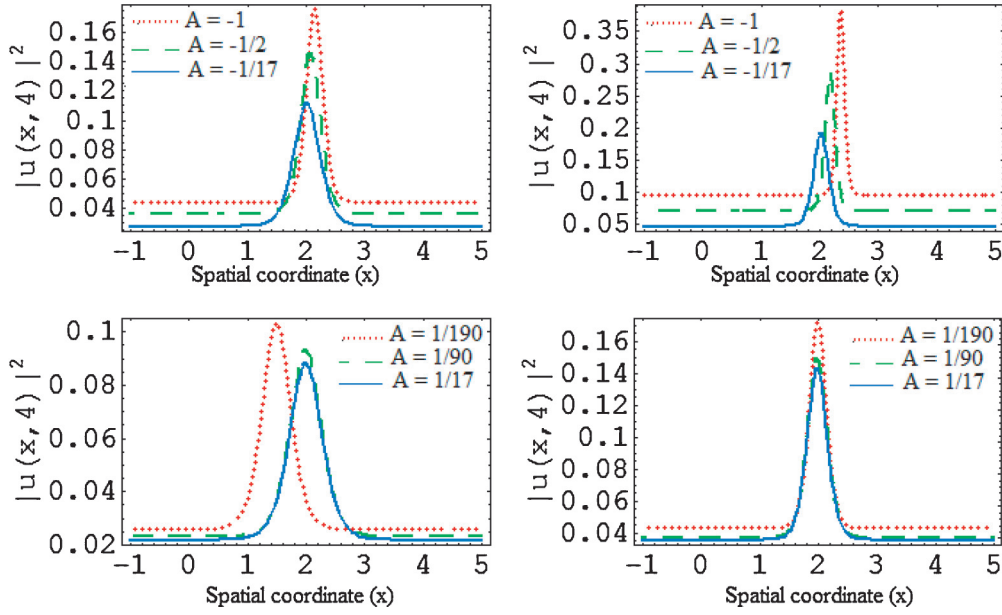


FIG. 9. (Color online) Density $|u(x,t)|^2$ at time $t = 4$ (in units of $2/\omega_{\perp}$) for three values of the parameter A appearing in potential (30), showing the effect of A on the peak density. The top and bottom panels correspond to confining potential and repulsive potential, respectively, while the left and right panels are associated with broadening condensates (with $t^* = 10$) and BECs in a shrinking trap (with $t^* = -10$), respectively. Typical values of all other parameters are given in the text.

B. Examples of solitary-wave solutions under conditions $\tilde{\delta} \neq 0$, $\tilde{\epsilon} < 0$, and $g_2 = g_3 = 0$

In the present subsection, we give examples of solitary-wave solutions when $\tilde{\delta} \neq 0$, $\tilde{\epsilon} < 0$, and $g_2 = g_3 = 0$. As we will see in what follows, one of the particularities of the present special case is that a bright and a dark solitary waves can exist for the same values of parameters $\tilde{\alpha}$, $\tilde{\beta}$, and $\tilde{\gamma}$. According to Eq. (43), solving the system $g_1 = g_2 = 0$ for $\epsilon < 0$ and $\tilde{\delta} \neq 0$

yields

$$\begin{aligned} \tilde{\epsilon} &= \tilde{\epsilon}(\tilde{\alpha}, \tilde{\beta}, \tilde{\gamma}) \\ &= \frac{4\tilde{\beta}^2(3\tilde{\alpha}\tilde{\gamma} - 2\tilde{\beta}^2) - 3\tilde{\alpha}^2\tilde{\gamma}^2 \pm 8\tilde{\beta}(\tilde{\beta}^2 - \tilde{\alpha}\tilde{\gamma})\sqrt{\tilde{\beta}^2 - \tilde{\alpha}\tilde{\gamma}}}{\tilde{\alpha}^3}, \\ \tilde{\delta} &= \tilde{\delta}(\tilde{\alpha}, \tilde{\beta}, \tilde{\gamma}) = \frac{3\tilde{\alpha}\tilde{\beta}\tilde{\gamma} - 2\tilde{\beta}^3 \pm 2(\tilde{\beta}^2 - \tilde{\alpha}\tilde{\gamma})\sqrt{\tilde{\beta}^2 - \tilde{\alpha}\tilde{\gamma}}}{\tilde{\alpha}^2}, \end{aligned}$$

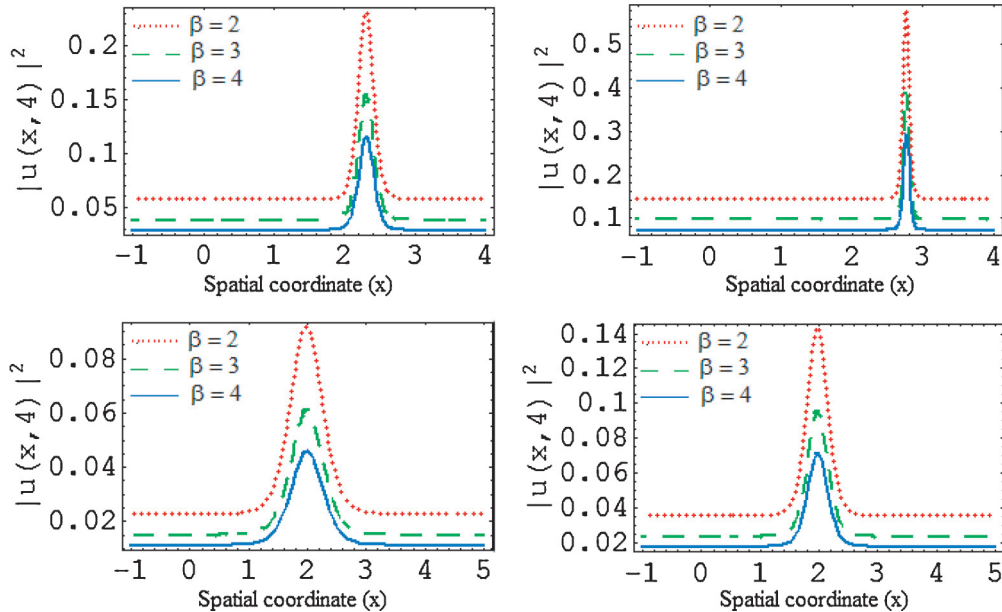


FIG. 10. (Color online) Density $|u(x,t)|^2$ at time $t = 4$ (in units of $2/\omega_{\perp}$) for three values of the imprint parameter β appearing in transformation (6b), showing the effect of β on the amplitude of the density. The upper and lower panels correspond to confining potential (with $A = -2$) and repulsive potential (with $A = 1/17$), respectively, while the left and right panels are associated with broadening condensates (with $t^* = 10$) and BECs in a shrinking trap (with $t^* = -10$), respectively. Typical values of all other parameters are given in the text.

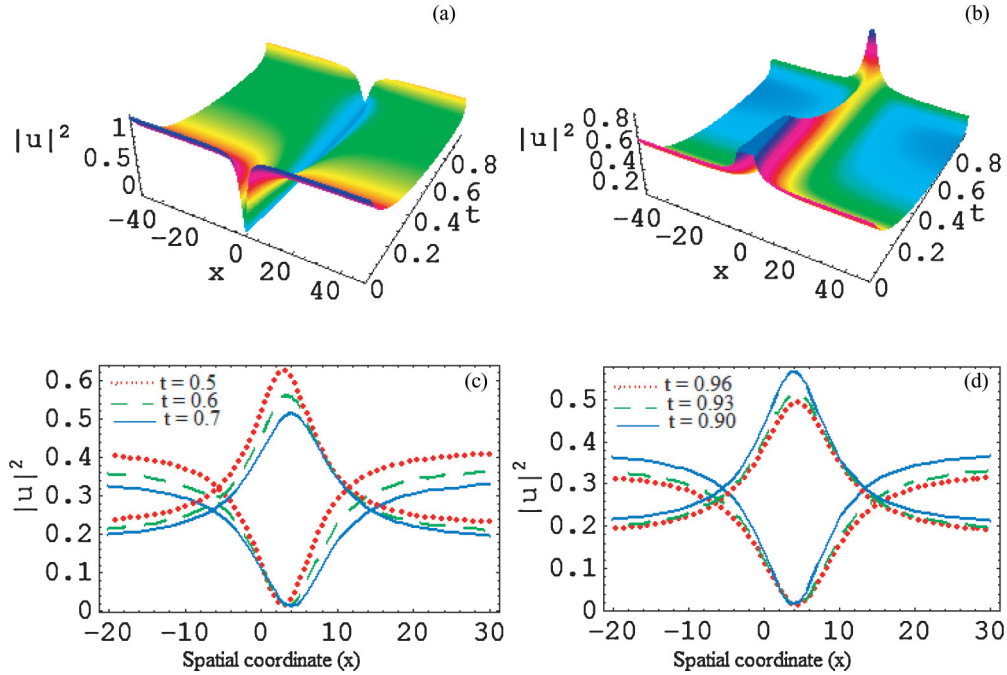


FIG. 11. (Color online) Plots of density $|u(x,t)|^2$ versus x (in units of a_{\perp}) and t (in units of $2/\omega_{\perp}$) for $\alpha(t) = (t-1)^{-2}/17$ with $\lambda = \lambda_0 = 1$, $k_0 = 0$, $\nu = 6$, $\phi_0 = 2.7813$ for the dark solitary wave (a), and $\phi_0 = 2.8013$ for the bright solitary wave (b). To generate these plots, we numerically solved Eq. (17) and system (18a)–(18d) with initial values $T(0) = 0$, $f(0) = 1.1$, $\eta(0) = 0$, $\ell(0) = 1$. Plot (a) is associated with the dark algebraic solitary-wave solution (47) (with sign “−”), while plot (b) corresponds to the bright algebraic solitary-wave solution (47) (with sign “+”). Plots (c) and (d) show the density profile for the dark and bright algebraic solitary wave at different times t , taken from the region of the positivity (c) and negativity (d) of the functional parameter $f(t)$.

if $\tilde{\beta}^2 - \tilde{\alpha}\tilde{\gamma} \geq 0$ and $4\tilde{\beta}^2(3\tilde{\alpha}\tilde{\gamma} - 2\tilde{\beta}^2) - 3\tilde{\alpha}^2\tilde{\gamma}^2 \pm 8\tilde{\beta}(\tilde{\beta}^2 - \tilde{\alpha}\tilde{\gamma})\sqrt{\tilde{\beta}^2 - \tilde{\alpha}\tilde{\gamma}} > 0$. Replacing $\tilde{\delta}$ and $\tilde{\epsilon}$ into Eq. (40) leads to the simple root $\zeta_0 = -\tilde{\alpha}^{-1}[\tilde{\beta} \pm 3\sqrt{\tilde{\beta}^2 - \tilde{\alpha}\tilde{\gamma}}]$ of

$$\zeta(z) = \frac{-\tilde{\alpha}[\tilde{\beta} \pm 3\sqrt{\tilde{\beta}^2 - \tilde{\alpha}\tilde{\gamma}}] + 4(\tilde{\alpha}\tilde{\gamma} - \tilde{\beta}^2)[- \tilde{\beta} \pm \sqrt{\tilde{\beta}^2 - \tilde{\alpha}\tilde{\gamma}}]z^2}{\tilde{\alpha}[\tilde{\alpha} - 4(\tilde{\beta}^2 - \tilde{\alpha}\tilde{\gamma})z^2]} \quad (47)$$

satisfying the needed condition of the non-negativity as soon as $\tilde{\beta} > 0$, $\tilde{\gamma} < 0$, $\tilde{\alpha}\tilde{\gamma} < \tilde{\beta}^2 < 9\tilde{\alpha}\tilde{\gamma}/8$. In solution (47), signs “−” and “+” are associated with the dark and bright solitary waves, respectively. By taking $\tilde{\alpha} = -1$, $\tilde{\beta} = 1$, and $\tilde{\gamma} = -8.1/9$, all the conditions of the existence of solution (47) for both signs “−” and “+” are satisfied. In other words, parameters $\tilde{\alpha} = -1$, $\tilde{\beta} = 1$, and $\tilde{\gamma} = -8.1/9$ together with $\tilde{\delta}(-1, 1, -8.1/9)$ and $\tilde{\epsilon}(-1, 1, -8.1/9) < 0$ define a dark and a bright solitary wave. The above values for $\tilde{\alpha}$, $\tilde{\beta}$, and $\tilde{\gamma}$ are obtained from system (41) for $\lambda = \lambda_0 = 1$, $k_0 = 0$, $\nu = 6$, $\phi_0 = 2.7813$ for the dark solitary wave, and $\phi_0 = 2.8013$ for the bright solitary wave. With these values of parameters, we show in Fig. 11 the density $|u(x,t)|^2$ corresponding to a dark (a) and a bright (b) algebraic solitary-wave solution for $\alpha(t) = (t-1)^{-2}/17$. The functional parameters $T(t)$, $f(t)$, $\ell(t)$, and $\eta(t)$ appearing in the density are obtained numerically by solving Eq. (17) and system (18a)–(18c) with initial conditions $T(0) = 0$, $f(0) = 1.1$, $\ell(0) = 1$, and $\eta(0) = 0$. With the initial datum $f(0) = 1.1$, function $f(t)$ changes its sign on $[0, 1[$, positive

the polynomial $f(\zeta)$. Inserting the above simple root ζ_0 into solution (45b) leads to the algebraic solitary waves

on $[0, t_0[$ and negative on $]t_0, 1[$. The change of the sign of $f(t)$, from positive to negative explains why the solitary wave propagates with a decreasing (increasing) amplitude on $[0, t_0[$ / $]t_0, 1[$. This situation is clearly seen in Figs. 11(c) and 11(d) showing the soliton profile at different times. It is also seen from Figs. 11(c) and 11(d) that the algebraic solitary waves move with an increasing (decreasing) peak in the region of positive (negative) $f(t)$. In the region of positive (negative) $f(t)$, the bright (dark) algebraic solitary wave move with a decreasing (increasing) width. Inversely, the dark (bright) algebraic solitary wave move with a decreasing (increasing) width in the region of negativity (positivity) of $f(t)$.

VI. SUMMARY AND DISCUSSION

In this work, we have examined the problem of modulational instabilities of plane waves in the context of the Gross–Pitaevskii equations with a time varying external potential. The motivation for this study was its direct link with the

“collisionally inhomogeneous” Bose–Einstein condensates which have a spatially modulated scattering length. To make possible the investigation of the MI for BECs with both attractive and repulsive two-body interactions, we first transformed the cubic GP equation into a cubic derivative NLS equation by suitably engineering the phase imprint on the old order parameter associated with the cubic GP equation. A modified lens transformation was then used to cast the problem in a rescaled space and time frame in which the cubic derivative NLS equation is converted into a similar equation without explicit spatial dependence. For the strength of the magnetic trap $\sim(t + t^*)^{-2}$ and a linear in the x temporal two-body interatomic interaction coefficient, the resulting growth rate of a purely growing MI is either constant or time varying. The effect of both the imprint parameter and the trap parameter t^* on the growth rate of the MI was investigated. In the case of constant gain, we have presented analytical solitary-wave-like solutions of the cubic GP equation and analyzed the effect of the above two parameters on the peak density.

Although we have investigated the problem of modulational instabilities of Stokes waves in the context of the GP equations

with a time varying external potential and, in some particular cases, have presented analytical solitonic-wave solutions, it is obvious that there are still many significant and important problems waiting for further investigations. Can we conclude on the stability of the analytical solitonic-wave solutions found in this paper? Does the imprint parameter affect the stability of solutions? Can one use the found analytical solutions to investigate the solitons’ collision? These are some of the pending problems! Our next challenge is the investigation of the stability of analytical solutions found in this work, and the effect of the imprint parameter on their stability.

ACKNOWLEDGMENTS

This work was supported by the Chinese Academy of Sciences Visiting Professorship for Senior International Scientists, the NKBRSCF under Grants No. 2011CB921502, No. 2012CB821305, No. 2009CB930701, and No. 2010CB922904, NSFC under Grants No. 10934010 and No. 60978019, and NSFC-RGC under Grants No. 11061160490 and No. 1386-N-HKU748/10.

-
- [1] M. H. Anderson, J. R. Ensher, M. R. Matthews, C. E. Wieman, and E. A. Cornell, *Science* **269**, 198 (1995); C. A. Sackett, J. J. Tollett, and R. G. Hulet, *Phys. Rev. Lett.* **75**, 1687 (1995); C. C. Bradley, C. A. Sackett, and R. G. Hulet, *ibid.* **78**, 985 (1997); K. B. Davis, M.-O. Mewes, M. R. Andrews, N. J. van Druten, D. S. Durfee, D. M. Kurn, and W. Ketterle, *ibid.* **75**, 3969 (1995).
- [2] B. P. Anderson, P. C. Haljan, C. A. Regal, D. L. Feder, L. A. Collins, C. W. Clark, and E. A. Cornell, *Phys. Rev. Lett.* **86**, 2926 (2001); Biao Wu, Jie Liu, and Qian Niu, *ibid.* **88**, 034101 (2002); C. K. Law, C. M. Chan, P. T. Leung, and M.-C. Chu, *ibid.* **85**, 1598 (2000).
- [3] E. Kengne and P. K. Talla, *J. Phys. B* **39**, 3679 (2006); S. Inouye, S. Gupta, T. Rosenband, A. P. Chikkatur, A. Görlitz, T. L. Gustavson, A. E. Leanhardt, D. E. Pritchard, and W. Ketterle, *Phys. Rev. Lett.* **87**, 080402 (2001).
- [4] K. E. Strecker, G. B. Partridge, A. G. Truscott, and F. G. Hulet, *Nature (London)* **417**, 150 (2002).
- [5] L. Khaykovich, F. Schreck, G. Ferrari, T. Bourdel, J. Cubizolles, L. D. Carr, Y. Castin, and C. Salomon, *Science* **296**, 1290 (2002).
- [6] S. J. Wang, C. L. Jia, D. Zhao, H. G. Luo, and J. H. An, *Phys. Rev. A* **68**, 015601 (2003).
- [7] M. R. Matthews, B. P. Anderson, P. C. Haljan, D. S. Hall, C. E. Wieman, and E. A. Cornell, *Phys. Rev. Lett.* **83**, 2498 (1999); K. W. Madison, F. Chevy, W. Wohlleben, and J. Dalibard, *ibid.* **84**, 806 (2000).
- [8] L. D. Carr and J. Brand, *Phys. Rev. Lett.* **92**, 040401 (2004).
- [9] M. Trippenbach, K. Góral, K. Rzazewski, B. A. Malomed, and Y. B. Band, *J. Phys. B* **33**, 4017 (2000); B. A. Malomed, D. J. Frantzeskakis, and P. G. Kevrekidis, *Phys. Rev. A* **70**, 043616 (2004); M. I. Merhasin, B. A. Malomed, and R. Driben, *J. Phys. B* **38**, 877 (2005); E. Kengne, R. Vaillancourt, and B. A. Malomed, *Int. J. Mod. Phys. B* **14**, 2211 (2010).
- [10] E. Kengne, R. Vaillancourt, and B. A. Malomed, *J. Phys. B* **41**, 205202 (2008); J. R. Abo-Shaeer, C. Raman, J. M. Vogels, and W. Ketterle, *Science* **292**, 476 (2001); P. Engels, I. Coddington, P. C. Haljan, and E. A. Cornell, *Phys. Rev. Lett.* **89**, 100403 (2002); E. Kengne, X. X. Liu, B. A. Malomed, S. T. Chui, and W. M. Liu, *J. Math. Phys.* **49**, 023503 (2008).
- [11] L. Li, Z. Li, B. Malomed, D. Mihalache, and W. Liu, *Phys. Rev. A* **72**, 033611 (2005); L. Li, B. A. Malomed, D. Mihalache, and W. M. Liu, *Phys. Rev. E* **73**, 066610 (2006).
- [12] Z. Rapti, P. G. Kevrekidis, A. Smerzi, and A. R. Bishop, *J. Phys. B* **37**, S257 (2004).
- [13] J. Belmonte-Beitia, V. M. Pérez-García, and V. Vekslerchik, *Chaos Solitons Fractals* **32**, 1268 (2007); G. R. Jin, C. K. Kim, and K. Nahm, *Phys. Rev. A* **72**, 045601 (2005).
- [14] F. Dalfovo, S. Giorgini, L. Pitaevskii, and S. Stringari, *Rev. Mod. Phys.* **71**, 463 (1999).
- [15] S. Burger, K. Bongs, S. Dettmer, W. Ertmer, and K. Sengstock, *Phys. Rev. Lett.* **83**, 5198 (1999).
- [16] J. Denschlag, J. E. Simsarian, D. L. Feder, Charles W. Clark, L. A. Collins, J. Cubizolles, L. Deng, E. W. Hagley, K. Helmerson, W. P. Reinhardt, S. L. Rolston, B. I. Schneider, and W. D. Phillips, *Science* **287**, 97 (2000).
- [17] Z. X. Liang, Z. D. Zhang, and W. M. Liu, *Phys. Rev. Lett.* **94**, 050402 (2005).
- [18] G. Theocharis, Z. Rapti, P. G. Kevrekidis, D. J. Frantzeskakis, and V. V. Konotop, *Phys. Rev. A* **67**, 063610 (2003).
- [19] L. A. Ostrovskii, *Zh. Eksp. Teor. Fiz.* **51**, 1189 (1966) [*Transl. Sov. Phys. JETP* **24**, 797 (1967)].
- [20] T. Taniuti and H. Washimi, *Phys. Rev. Lett.* **21**, 209 (1968); A. Hasegawa, *ibid.* **24**, 1165 (1970).
- [21] M. B. Dahan, E. Peik, J. Reichel, Y. Castin, and C. Salomon, *Phys. Rev. Lett.* **76**, 4508 (1996).
- [22] G. P. Agrawal, *Nonlinear Fiber Optics* (Academic, San Diego, 2001).
- [23] I. Kourakis, P. K. Shukla, M. Marklund, and L. Stenflo, *Eur. Phys. J. B* **46**, 381 (2005).
- [24] L. Wu, J. F. Zhang, and L. Li, *New J. Phys.* **9**, 69 (2007).

- [25] A. Mohamadou, E. Wamba, S. Y. Doka, T. B. Ekogo, and T. C. Kofane, *Phys. Rev. A* **84**, 023602 (2011).
- [26] A. Rogister, *Phys. Fluids* **14**, 2733 (1971); E. Mjølhus, *J. Plasma Phys.* **16**, 321 (1976); K. Mio, T. Ogino, K. Minami, and S. Takeda, *J. Phys. Soc. Jpn.* **41**, 265 (1976); F. Verheest and B. Buti, *J. Plasma Physics* **47**, 15 (1992).
- [27] M. S. Ruderman, *Phys. Plasmas* **9**, 2940 (2002).
- [28] N. Tzoar and M. Jain, *Phys. Rev. A* **23**, 1266 (1981); D. Anderson and M. Lisak, *ibid.* **27**, 1393 (1983).
- [29] A. Kundu, *J. Math. Phys.* **25**, 3433 (1984); R. Radhakrishnan, A. Kundu, and M. Lakshmanan, *Phys. Rev. E* **60**, 3314 (1999).
- [30] H. R. Brand and R. J. Deissler, *Phys. Rev. Lett.* **63**, 2801 (1989).
- [31] R. J. Deissler and H. R. Brand, *Phys. Lett. A* **130**, 2801 (1988).
- [32] Ł. Dobrek, M. Gajda, M. Lewenstein, K. Sengstock, G. Birkel, and W. Ertmer, *Phys. Rev. A* **60**, R3381 (1999).
- [33] S. Inouye, M. R. Andrews, J. Stenger, H. J. Miesner, D. M. Stamper-Kurn, and W. Ketterle, *Nature (London)* **392**, 151 (1998).
- [34] S. L. Cornish, S. T. Thompson, and C. E. Wieman, *Phys. Rev. Lett.* **96**, 170401 (2006).
- [35] M. Bartenstein, A. Altmeyer, S. Riedl, S. Jochim, C. Chin, J. Denschlag, and R. Grimm, *Phys. Rev. Lett.* **92**, 203201 (2004).
- [36] F. Kh. Abdullaev, J. G. Caputo, R. A. Kraenkel, and B. A. Malomed, *Phys. Rev. A* **67**, 013605 (2003).
- [37] H. Saito and M. Ueda, *Phys. Rev. Lett.* **90**, 040403 (2003).
- [38] P. G. Kevrekidis, G. Theocharis, D. J. Frantzeskakis, and B. A. Malomed, *Phys. Rev. Lett.* **90**, 230401 (2003).
- [39] G. Theocharis, P. Schmelcher, P. G. Kevrekidis, and D. J. Frantzeskakis, *Phys. Rev. A* **72**, 033614 (2005); F. Kh. Abdullaev and M. Salerno, *J. Phys. B* **36**, 2851 (2003); M. I. Rodas-Verde, H. Michinel, and V. M. Pérez-García, *Phys. Rev. Lett.* **95**, 153903 (2005); A. V. Carpentier, H. Michinel, M. I. Rodas-Verde, and V. M. Pérez-García, *Phys. Rev. A* **74**, 013619 (2006).
- [40] S. Eriksson, M. Trupke, H. F. Powell, D. Sahagun, C. D. J. Sinclair, E. A. Curtis, B. E. Sauer, E. A. Hinds, Z. Moktadir, C. O. Gollasch, and M. Kraft, *Eur. Phys. J. D* **35**, 135 (2005); F. Kh. Abdullaev, Yu. V. Bludov, S. V. Dmitriev, P. G. Kevrekidis, and V. V. Konotop, *Phys. Rev. E* **77**, 016604 (2008).
- [41] V. M. Pérez-García, H. Michinel, and H. Herrero, *Phys. Rev. A* **57**, 3837 (1998).
- [42] A. D. Jackson, G. M. Kavoulakis, and C. J. Pethick, *Phys. Rev. A* **58**, 2417 (1998); P. Ping and L. Guan-Qiang, *Chin. Phys. B* **41**, 3221 (2009); A. Gammal, T. Frederico, L. Tomio, and Ph. Chomaz, *J. Phys. B* **33**, 4053 (2000).
- [43] A. L. Fetter and J. D. Walecka, *Quantum Theory of Many-Particle Systems* (McGraw-Hill, New York, 1971).
- [44] L. Salasnich, A. Parola, and L. Reatto, *Phys. Rev. A* **65**, 043614 (2002).
- [45] U. Al. Khawaja, *J. Phys. A* **39**, 9679 (2006).
- [46] V. R. Kumar, R. R. Adha, and M. W. Adati, *J. Phys. Soc. Jpn.* **79**, 074005 (2010).
- [47] A. J. Leggett, *Rev. Mod. Phys.* **73**, 307 (2001).
- [48] V. V. Konotop and M. Salerno, *Phys. Rev. A* **65**, 021602(R) (2002).
- [49] W. Schöpf and W. Zimmermann, *Europhys. Lett.* **8**, 41 (1989); *Phys. Rev. E* **47**, 1739 (1993); J. Duan and P. Holmes, *Proc. Edinburgh Math. Soc.* **2**, 77 (1995).
- [50] E. Kengne and W. M. Liu, *Phys. Rev. E* **73**, 026603 (2006); E. Kengne, A. Lakhssassi, T. Nguyen-Ba, and R. Vaillancourt, *Can. J. Phys.* **88**, 55 (2010).
- [51] D. Schumayer and B. Apagyi, *Phys. Rev. A* **65**, 053614 (2002).
- [52] C. Sulem and P. L. Sulem, *The Nonlinear Schrödinger Equation* (Springer-Verlag, New York, 1999).
- [53] C. I. Siettos, I. G. Kevrekidis, and P. G. Kevrekidis, *Nonlinearity* **16**, 497 (2003).
- [54] E. T. Whittaker and G. N. Watson, *A Course of Modern Analysis* (Cambridge University Press, Cambridge, 1927).
- [55] K. Weierstrass, *Mathematische Werke V* (Johnson, New York, 1915).
- [56] K. Chandrasekharan, *Elliptic Functions* (Springer, Berlin, 1985).
- [57] H. W. Schürmann, *Phys. Rev. E* **54**, 4312 (1996).
- [58] P. G. Drazin, *Soliton*, Lecture Note Series 85 (Cambridge University Press, Cambridge, London, 1983).
- [59] H. W. Schürmann and S. V. Serov, *J. Math. Phys.* **45**, 2181 (2004).
- [60] J. F. Zhang, C. Q. Dai, Q. Yang, and J. M. Zhu, *Opt. Commun.* **252**, 408 (2005).